EFFICENCY DEFINITIONS OF HYDRAULIC TRANSFORMERS AND FIRST TEST RESULTS OF THE FLOATING CUP TRANSFORMER (FCT80)

Robin Mommers*, Sef Achten, Jeroen Potma, Jasper Achten, Peter Achten

INNAS B.V., Nikkelstraat 15, 4823AE Breda, The Netherlands

* E-mail address: rmommers@innas.com

ABSTRACT

The FCT80 is a new hydraulic transformer, based on the floating cup principle. The transformer has valve plates with three ports, and is controlled by means of setting the rotational position of these valve plates. Contrary to hydraulic pumps and motors, there are no standardised efficiency definitions for this type of integrated transformers. In this paper, general definitions for efficiency and power loss for hydraulic transformers are proposed, which also take the compressibility of the oil into account. This paper also describes and presents the first test results of the overall efficiency of the FCT80.

Keywords: hydraulic transformer, efficiency, floating cup

1. INTRODUCTION

It is well known, that fluid power systems are not very energy efficient. In [1], the authors estimate an average overall hydraulic system efficiency of 22%. Three significant factors for a low overall system efficiency are:

- dissipative control by means of proportional valves
- inability to recuperate energy
- inefficient operating conditions for the main (variable displacement) supply pump

Common pressure rail (CPR) systems and secondary control provide a solution to these three issues [2]. Several studies have concluded that the introduction of such system architectures can reduce the energy consumption of hydraulic systems by 30% to over 50% compared to load-sense systems [3–7]. Hydraulic transformers can be essential for the realisation of CPR-systems.

Hydraulic transformers provide a non-dissipative way to control the power delivery to the individual work functions. Furthermore, transformers can recuperate energy, which can then be used by other loads or stored in hydraulic accumulators. Additionally, by using accumulators, the energy source (the supply pump) is decoupled from the loads. Therefore, the inefficiently operated, variable displacement supply pump, can be replaced by a more efficient (and less expensive) constant displacement pump. Finally, because of the drastic reduction in losses, less cooling capacity will need to be installed to control the fluid temperature.

While several prototype hydraulic transformers have been developed and tested [8–10], there currently is no hydraulic transformer that is commercially available. Therefore, there is no standard definition for the efficiency of these machines. In this study, a definition for the power loss and efficiency of hydraulic transformers is derived that also takes into account the compressibility of the oil.

Furthermore, an attempt is made to divide these losses into flow and torque losses, based on the theoretical displacement of the transformer. This analysis provides a good theoretical understanding of the basic operation of a hydraulic transformer, as well as give some indication of where losses in such a device can be expected. However, it will be shown that this theoretical division cannot provide an accurate representation of the different losses in an actual transformer.

The derived definitions for overall power loss and efficiency are used to map the performance of a new hydraulic transformer prototype. This 80 cc/rev Floating Cup type hydraulic transformer has been designed and developed by Innas [11].

2. EFFICIENCY DEFINITION

2.1. Hydraulic power

The classical definition of hydraulic power is simply the product of pressure p and flow rate Q. Several studies have suggested that this definition is no longer sufficient, and the hydraulic power should also include a small amount of compression energy [12–15]. According to [12], the hydraulic power P in a mass flow, including compression energy, can be approximated using (1).

$$P = pQ\left(1 + \frac{p}{2\overline{K}_s}\right) \tag{1}$$

with \overline{K}_s the average isentropic bulk modulus of the oil. Please note that (1) describes the hydraulic power in the fluid with respect to absolute zero pressure. Since the pressure in a hydraulic system will never drop down to absolute zero, there is always a certain amount of hydraulic power present in the oil. Therefore the power consumption of a hydraulic component is always defined as a change in power, as will be shown next.

2.2. Motors and pumps

Figure 1a shows a hydraulic motor without an external leak port, that is connected to a supply pressure p_1 and an output pressure p_0 ($p_1 > p_0$). Since the output pressure is not absolute zero pressure ($p_1 > 0$), the hydraulic power that is consumed by this motor, P_{in} , is found to be the difference between the hydraulic power that is available at the input port and the power that remains in the fluid that leaves the motor at the output port.

$$P_{in} = p_1 Q_1 \left(1 + \frac{p_1}{2\overline{K}_s} \right) - p_0 Q_0 \left(1 + \frac{p_0}{2\overline{K}_s} \right) \tag{2}$$

The motor converts this hydraulic power into mechanical power in the form of torque and rotary speed (T, ω) , respectively). In [14], the authors show that, at least for a hydrostatic machine without external leak flow, the hydraulic power can be defined with respect to any reference pressure level. Choosing p_0 as the reference pressure results in (3).

$$P_{in} = \hat{p}_1 Q_1 \left(1 + \frac{\hat{p}_1}{2\overline{K}_s} \right), \quad \text{with } \hat{p}_1 = p_1 - p_0$$
 (3)

For a pump, the process of power conversion is reversed: mechanical power is converted to hydraulic power. **Figure 1b** shows a hydraulic pump without an external leak port. The hydraulic output power of this pump, P_{out} , is given by (4).

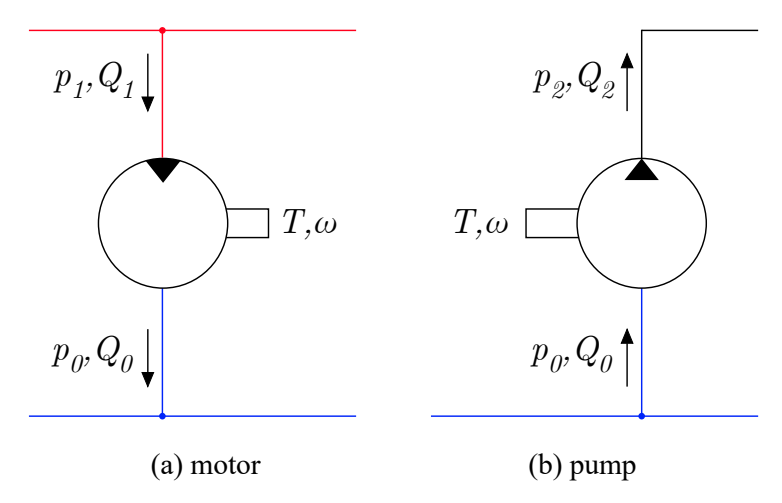


Figure 1: A hydraulic motor converts hydraulic power into mechanical power, a pump converts mechanical power into hydraulic power.

$$P_{out} = \hat{p}_2 Q_2 \left(1 + \frac{\hat{p}_2}{2\overline{K}_S} \right), \quad \text{with } \hat{p}_2 = p_2 - p_0$$
 (4)

where p_2 and Q_2 are the pressure and flow rate at the discharge side of the pump.

2.3. Hydraulic transformers

Traditionally, the mechanical input power for a pump is supplied by an internal combustion engine, or an electric motor, while the output power of a motor can be used at a work function. The basic idea of a hydraulic transformer is to use hydraulic power to generate mechanical power, that is then converted back to hydraulic power again. In that sense, a hydraulic transformer can be seen as a combination of a motor and a pump, as is illustrated in **Figure 2b**.

Figure 2a shows the symbol for a hydraulic transformer. To function correctly, such a device is part of a CPR-system. The CPR-system consist of a high-pressure rail (HPR), at pressure p_1 , and a low-pressure rail (LPR), at pressure p_0 . A transformer uses the pressure difference between these two rails to control the power that is send to a load via the third port, at pressure p_2 . The direction of flow rate Q at the different ports is not fixed; it can flow in either direction. In this study, flow rates are defined positive when oil flows into the transformer.

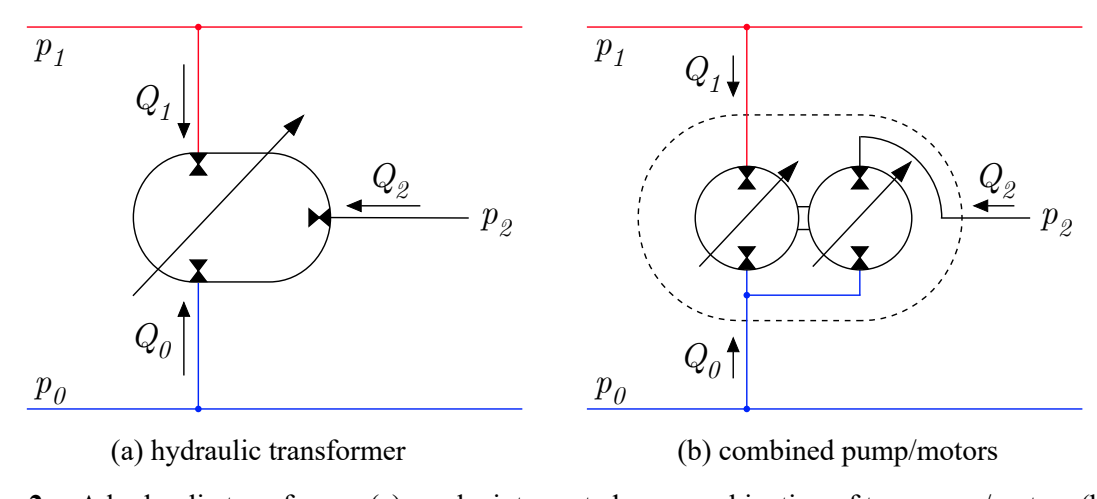


Figure 2: A hydraulic transformer (a) can be interpreted as a combination of two pump/motors (b), and is connected to a CPR-system and a load.

Note that the only difference between the input power for a motor, from (3), and the output power for a pump, from (4), is the direction of the flow rate. Since the transformer is able to deliver power to the load $(Q_2 < 0)$, as well as recuperate energy from the load back to the CPR-system $(Q_2 > 0)$, there is no clear definition of input or output power. Instead, we get the following equilibrium of power:

$$\hat{p}_1 Q_1 \left(1 + \frac{\hat{p}_1}{2\overline{K}_s} \right) + \hat{p}_2 Q_2 \left(1 + \frac{\hat{p}_2}{2\overline{K}_s} \right) = P_{loss}$$
 (5)

in which P_{loss} is the total amount of power loss within the transformer. Since the efficiency η is the ratio between output and input power, we need to differentiate between the two modes of operation.

$$\eta = \frac{P_{out}}{P_{in}} = \begin{cases}
-\frac{\hat{p}_2 Q_2 \left(1 + \frac{\hat{p}_2}{2\overline{K}_S}\right)}{\hat{p}_1 Q_1 \left(1 + \frac{\hat{p}_1}{2\overline{K}_S}\right)}, & \text{when } Q_2 \le 0 \\
-\frac{\hat{p}_1 Q_1 \left(1 + \frac{\hat{p}_1}{2\overline{K}_S}\right)}{\hat{p}_2 Q_2 \left(1 + \frac{\hat{p}_2}{2\overline{K}_S}\right)}, & \text{when } Q_2 > 0
\end{cases}$$
(6)

This definition implies that, in order to calculate the efficiency of a transformer, we need to measure the flow rate at ports 1 and 2, and the pressure at ports 0, 1, and 2.

2.4. Previous efficiency definitions

There are different definitions of the efficiency of hydraulic transformers to be found in literature [9,10,16,17]. Apart from the fact that these studies do not include the compressibility of the oil, there are some other notable differences.

In these studies, the transformer is isolated from the rest of the CPR-system. The absolute pressure level (p_i) is used instead of the pressure level with respect to the LPR-pressure (\hat{p}_i) . In doing so, the flow rate at port 0 is considered to have usable hydraulic power as well and needs to be included in the definitions for power loss and efficiency. In cases where $p_2 < p_1$, we find a positive flow rate into port 0 $(Q_0 > 0)$ so this is considered input power. In cases where $p_2 > p_1$, the direction of the flow rate at port 0 can change $(Q_0 < 0)$. In these cases, the hydraulic power at port 0 is considered an output power.

In [17], a second definition is given where the author considers the transformer to be part of a hydrostatic transmission. The derived efficiency definition is therefore similar to (6). This approach is based on the idea that the transformer cannot extract any more energy from the oil once it is at pressure level p_0 , so this is the minimum energy state of the CPR-system.

3. DIVISION OF LOSSES

To better understand where the power loss from (5) is coming from, the combined pump/motor interpretation shown in **Figure 2b** is used again. In this section we assume that the transformer is delivering power to a load $(Q_1 > 0, Q_2 < 0, \omega > 0)$. The machine that is connected to p_1 therefore acts as a motor, and the machine connected to p_2 acts as a pump. The derivations in this section are made under the assumption of a constant bulk modulus and a linear compression ratio. In other words, areas in pV-diagrams are approximated by simple triangles and rectangles.

3.1. Theoretical single piston displacement

Figure 3 shows the ideal pV-diagram of a single piston in both of the machines, including compressibility effects as also derived in [12–15]. In these figures, ΔV_i describes the volume that a single piston displaces from port i.

$$\Delta V_1 = V_{1,max} \left(1 - \frac{\hat{p}_1}{\overline{K}_s} \right) - V_{1,min} \tag{7}$$

$$\Delta V_2 = V_{2,min} - V_{2,max} \left(1 - \frac{\hat{p}_2}{\overline{K}_s} \right) \tag{8}$$

where $V_{i,min}$ and $V_{i,max}$ are the minimum and maximum geometric piston volume (for the current displacement) of machine *i*. Please note that $\Delta V_2 < 0$ in order to agree with the sign convention that was introduced in the previous section.

3.2. Flow rate loss

The displacement volume per piston per revolution, as described in (7) and (8), can be used to derive a theoretical flow rate $Q_{i,th}$.

$$Q_{i,th} = \frac{\omega Z_i}{2\pi} \Delta V_i = \omega D_i \tag{9}$$

where z_i is the number of pistons and D_i is the displacement of the full machine at port i. When measuring the flow rate for an actual transformer, the flow rate at port i will not be ideal.

$$Q_i = Q_{i,th} + Q_{i,loss} = \omega D_i + Q_{i,loss}, \quad \text{with } Q_{i,loss} \ge 0$$
 (10)

where $Q_{i,loss}$ is the difference between the measured flow rate Q_i and the ideal flow rate. If there is a lot of leakage at the motor, the flow rate over the motor is much higher than the theoretical flow rate at the current rotor speed. The hydraulic power in this leaked oil is not used to propel the pump, and is thus lost. Similarly, if there is a lot of leakage at the pump, there will be less fluid leaving the

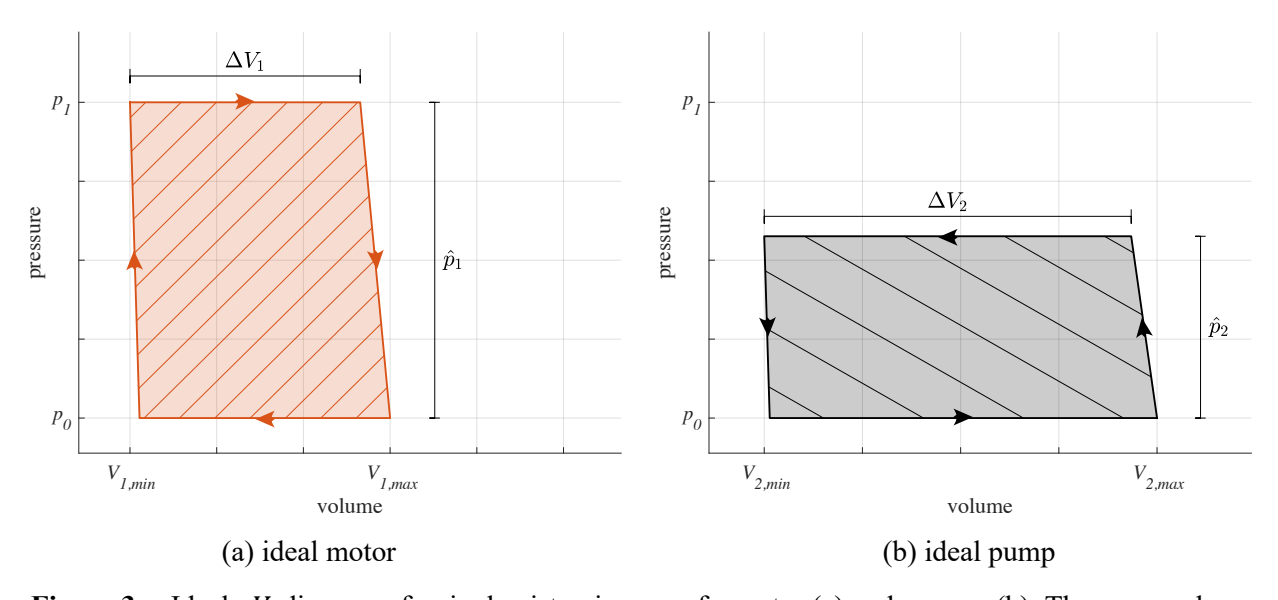


Figure 3: Ideal *pV*-diagram of a single piston in case of a motor (a) and a pump (b). The arrows show the direction through which the diagram is followed for a positive rotational speed. N.B. The bulk modulus has been decreased significantly to show the effect of compressibility.

transformer than the theoretical flow rate. Some of the torque that was used to propel the pump has been converted to hydraulic power that then has leaked back to reference pressure p_0 instead of leaving the transformer to move a work function. This is also a loss.

3.3. Torque loss

The area that the pV-diagram of a piston encircles can be used to calculate the torque T_i of machine i. From **Figure 3**, the torque is found to be:

$$T_{i} = \frac{z_{i}}{2\pi} \int p dV = \frac{z_{i}}{2\pi} \hat{p}_{i} \Delta V_{i} \left(1 + \frac{\hat{p}_{i}}{2\overline{K}_{s}} \right) = \hat{p}_{i} D_{i} \left(1 + \frac{\hat{p}_{i}}{2\overline{K}_{s}} \right)$$

$$\tag{11}$$

When a transformer is in steady state, i.e. the transformer is not accelerating, the total torque on the shaft will be 0. Assuming that the transformer has some internal torque loss, we get the following equilibrium.

$$\hat{p}_1 D_1 \left(1 + \frac{\hat{p}_1}{2\overline{K}_S} \right) + \hat{p}_2 D_2 \left(1 + \frac{\hat{p}_2}{2\overline{K}_S} \right) = T_{loss}$$
 (12)

For an ideal transformer ($T_{oss} = 0$), the motor torque is equal to the additive inverse of the pump torque. When the motor and pump are set to a certain displacement, and the CPR-system is at a certain pressure difference \hat{p}_1 , the only variable in (12) is the output pressure \hat{p}_2 . This means that in order to balance the torque on the rotor, the output pressure changes.

3.4. Comparing losses

Since the flow rate loss and the torque loss have different units, it is difficult to compare the size of the two. Substitution of (10) in (5) results in (13).

$$P_{loss} = \hat{p}_{1}(\omega D_{1} + Q_{1,loss}) \left(1 + \frac{\hat{p}_{1}}{2\overline{K}_{s}} \right) + \hat{p}_{2}(\omega D_{2} + Q_{2,loss}) \left(1 + \frac{\hat{p}_{2}}{2\overline{K}_{s}} \right)$$

$$= T_{loss}\omega + Q_{1,loss}\hat{p}_{1} \left(1 + \frac{\hat{p}_{1}}{2\overline{K}_{s}} \right) + Q_{2,loss}\hat{p}_{2} \left(1 + \frac{\hat{p}_{2}}{2\overline{K}_{s}} \right)$$

$$= P_{loss,T} + P_{loss,Q_{1}} + P_{loss,Q_{2}}$$
(13)

Where $P_{loss,T}$, P_{loss,Q_1} , and P_{loss,Q_2} are the power losses associated with the torque loss, and flow rate losses from port 1 and 2.

3.5. Innas Hydraulic Transformer principle

The Innas Hydraulic Transformer (IHT) principle is different from the example above in that it provides an integrated combination of the motor and pump from **Figure 3** into a single rotation group [8]. **Figure 4** shows an example of the pV-diagram of a single piston in such a machine. Starting in the top left corner of **Figure 4a**, the piston is connected to p_1 and the chamber volume is minimal, V_{min} . Following the direction of the arrow, the chamber volume starts expanding, drawing in oil from the HPR. At some point, the valve plate disconnects the piston from p_1 and connects to p_0 , after which the piston expands further to its maximum volume V_{max} . At this point, the direction changes, and the chamber volume starts to decrease while the piston is still connected to p_0 . Shortly thereafter, the valve plate disconnects the piston from p_0 and connects to p_2 , where the oil is displaced to the

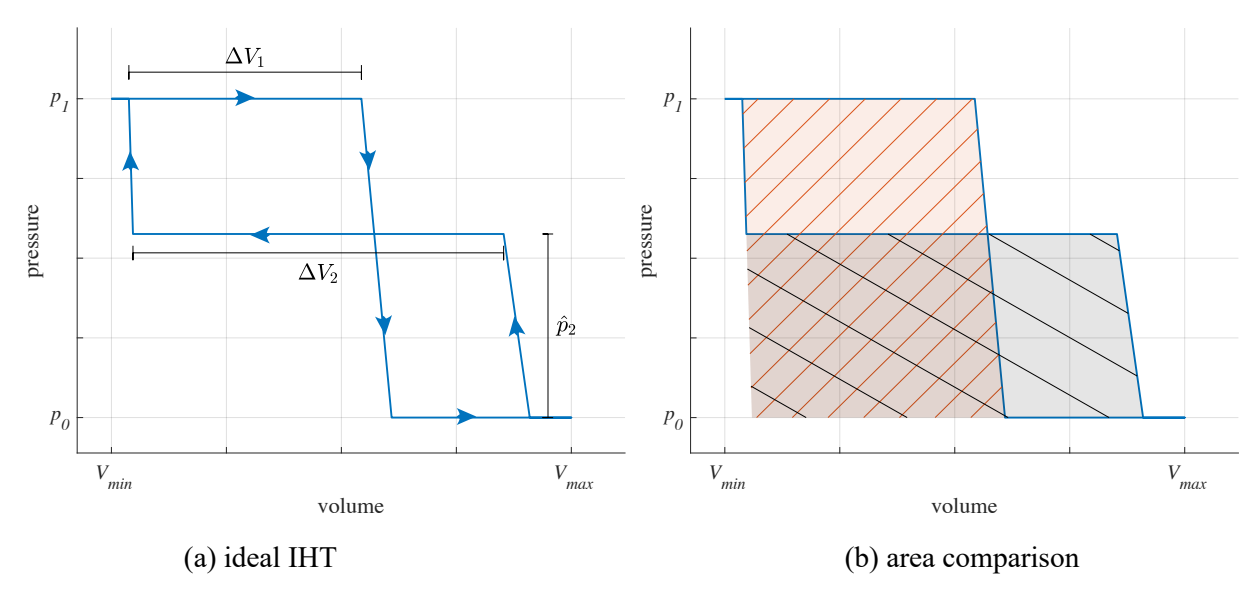


Figure 4: Ideal pV-diagram of a single piston in a transformer that uses the IHT principle.

work function. Finally, near the end of the discharge stroke, the piston is connected to p_1 again, after which the piston volume decreases further to its minimum volume again.

While the motor and pump action in an IHT do not occur in different machines, we can still define the displaced volume on ports 1 and 2, as is shown in **Figure 4a**. Therefore, equations (7) to (13) still hold. **Figure 4b** shows that the total area of the IHT pV-diagram can be divided into an equal sized motoring and pumping part, similar to the diagrams shown in **Figure 3**.

3.6. The problem with measuring displacement volume

Equations (10) and (12) define a flow rate loss and a torque loss, based on the theoretical displacement volume at ports 1 and 2 of the transformer. For pumps and motors, there is a well-known method for determining the displacement volume [18]. This method relies on measuring the flow rate at the high-pressure port of the unit at different operating speeds and different pressure levels. These measured flow rates are then extrapolated such that a displacement volume is derived for 0 rpm and 0 bar operating conditions. This method cannot be used for hydraulic transformers that are based on the IHT principle. The main reason for this, is that the pressure at port 2 cannot be chosen arbitrarily, since it is coupled to the ratio of ΔV_1 and ΔV_2 . In other words, the displacement volume is different for each pressure level that is measured.

Furthermore, the *pV*-diagrams shown in **Figure 3** and **Figure 4** describe the ideal case, with perfect expansion and compression of the oil. **Figure 5a** shows the *pV*-diagram of a single piston, from a simulation model of the prototype transformer that is discussed in the next section. In this model, the transformer has some rotor friction, but has no leakage.

From **Figure 5a**, it is less clear how the losses are related to the geometric values of ΔV_1 and ΔV_2 . For example, at corner a in **Figure 5a**, the pressure in the chamber starts to decrease before the chamber is at the ideal volume, since the flow area between port 1 and the piston chamber has to close at this point. Therefore, this chamber has effectively displaced less fluid from port 1. If the geometric value of ΔV_1 is used in (9) and (10), we find that the flow rate at port 1 is less than the ideal flow rate. This would result in a negative flow loss at port 1 ($Q_{1,loss} < 0$) for this machine. Something similar occurs for the displacement at port 2.

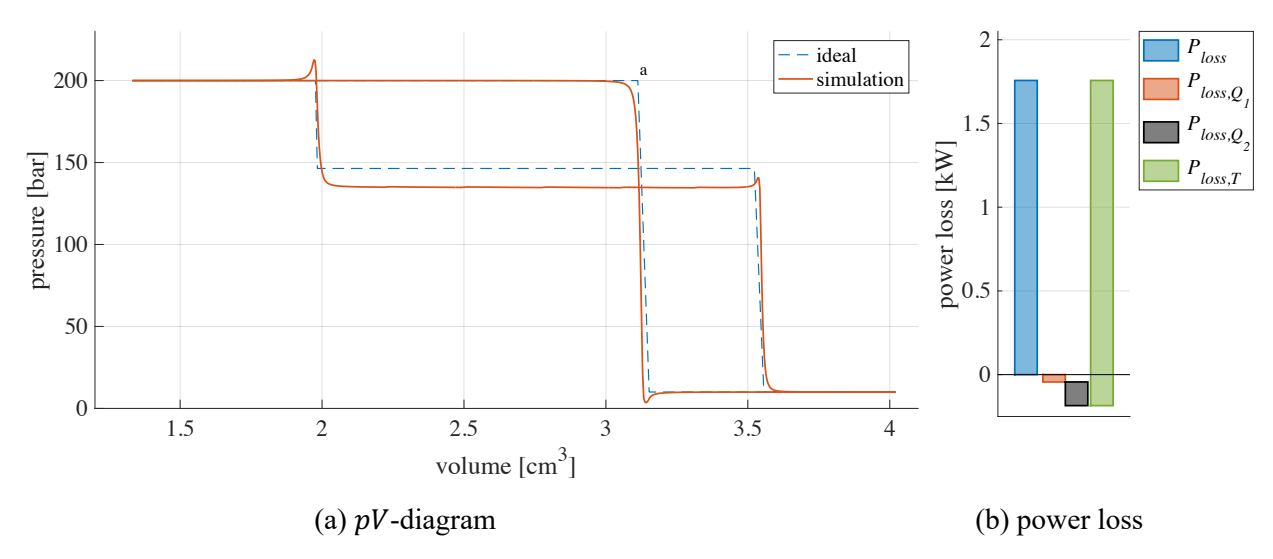


Figure 5: Ideal versus simulated *pV*-diagram for a piston in the FCT80 in (a) and division of power loss in (b), simulated at control angle 25°, and roughly 1500 rpm.

Figure 5b shows an example of the derived division of power loss for this simulated situation. The negative flow losses are countered by an exaggeration of the torque losses. Since the effective displacement at the ports is found to be less than the geometrical displacement volume, we calculate a higher torque loss in (12). The result is a torque loss that is larger than the overall power loss.

3.7. Conclusion

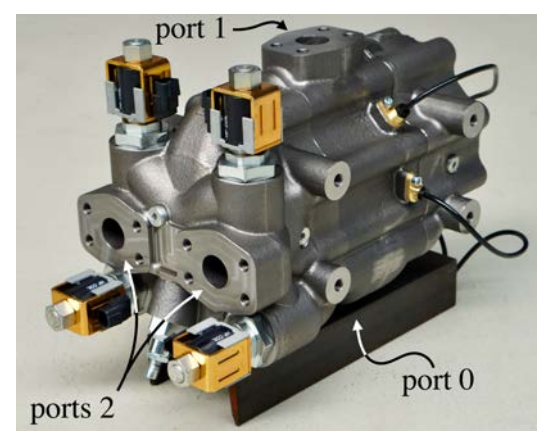
The theoretical division of losses for a hydraulic transformer can be made using pV-diagrams of ideal machines. This can be very useful in understanding the basic operating principle of hydraulic power transformation. Unfortunately, this division relies heavily on a good understanding of the displacement volume of the transformer at ports 1 and 2 at all possible operating conditions. To the authors knowledge, there is no known method to measure this displacement volume at the different operating conditions of an IHT.

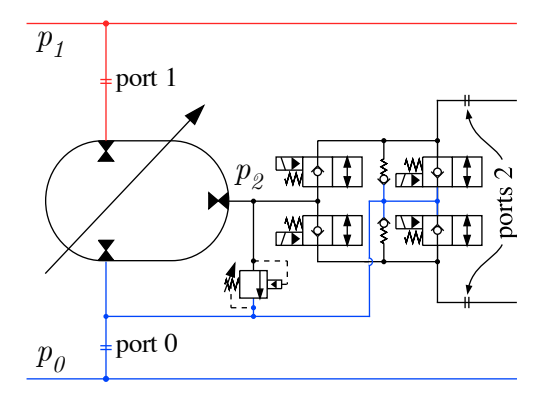
4. FCT80

A new 80 cc/rev floating cup type hydraulic transformer (FCT80) has been designed by Innas [11]. **Figure 6a** shows a photo of the machined and assembled prototype. In the shown orientation, port 0 is not visible as it is on the bottom of the housing, and port 1 is found on the top. The front of the housing has two load ports 2. These two ports can for example be connected to either side of a hydraulic cylinder. There are four solenoid valves that can then be used to control which side of the cylinder is connected to p_2 and which side is connected to p_0 , as is shown in hydraulic circuit in **Figure 6b**.

At high flow rates, the pressure difference over the control valves can become significant. To reduce the risk of cavitation at the port that is connected to p_0 , there are two built-in check valves parallel to the solenoid valves. Furthermore, the circuit also shows an internal relief valve for safety reasons.

The FCT80 is controlled by an electric stepper motor, combined with a hydraulic servo motor [11]. In steady state conditions, this hydraulic servo motor will draw some high-pressure oil from the HPR, as it needs to deliver a certain continuous control torque while there is some internal leak flow. Since the motor is fed from within the transformer, this control power loss is automatically included in the overall efficiency measurements, in the form of a slightly higher flow rate at port 1. The power loss from the stepper motor will be negligible, as there is no continuous torque on the shaft of the stepper.





(a) photo of the FCT80 prototype

(b) hydraulic circuit of housing

Figure 6: The FCT80 prototype has two load ports, four control valves, two check valves, and a relief valve, all build into the housing.

5. TEST RESULTS

5.1. Test setup

The setup used to measure the performance of the FCT80 is shown in **Figure 7**. Several parameters are measured using the sensors that are listed in **Table 1**. The other components have been chosen such that the transformer can be operated in a steady state, i.e. constant pressure and flow rate on ports 0, 1, and 2.

The top left of **Figure 7** shows an electric motor that drives a 45 cc/rev pump. The output of this main pump is connected to port 1 of the FCT80. Between the pump and the transformer, there is a 5 L accumulator that is pre-charged at 157 bar. This part of the setup can be considered to be the HPR. The supply side of the pump is connected to port 0 of the FCT80. There is another 5 L accumulator between them, which is pre-charged to 4 bar. This part can be considered to be the LPR.

The speed of the main electric motor is controlled by the pressure measurement at port 1. The pressure in the LPR is maintained using a small charge pump in combination with a proportional valve. This is needed because for a different state of charge of the accumulators, there is a difference in total oil volume in the circuit. Additionally, the main pump has an external drain port (not shown in **Figure 7**) which also leaks some oil back to tank.

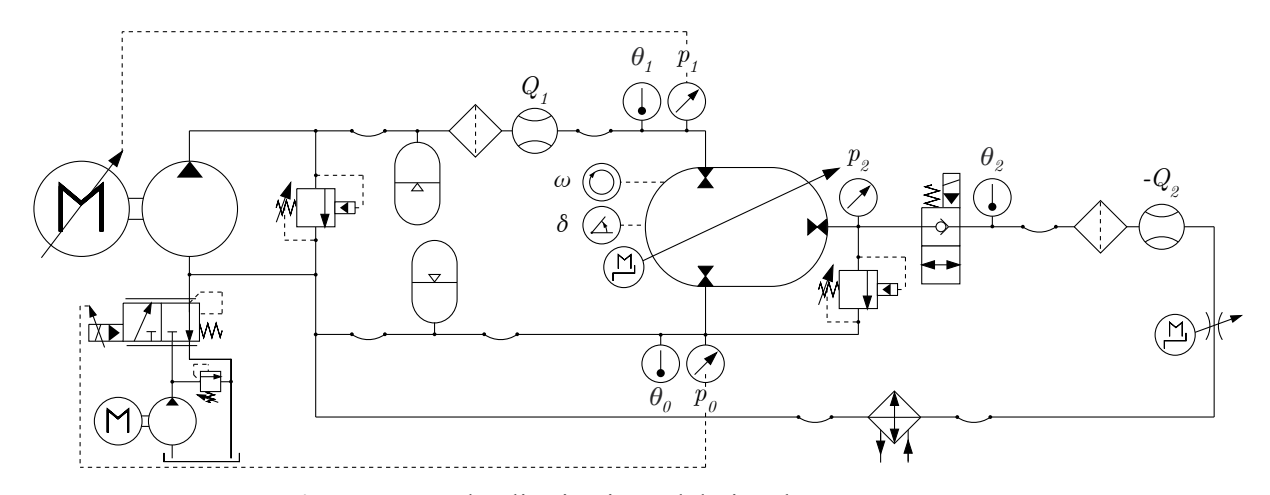


Figure 7: Hydraulic circuit used during the measurements.

Table 1: List of the sensors used in the transformer testbench.

variable	symbol	sensor	range	accuracy
control angle	δ	Micro-Epsilon ES-U2	0.2 to 2.2 mm	0.04 μm
high pressure	p_{1}, p_{2}	Honeywell STJE 7500 psig	0 to 517.1 bar	± 0.259 bar
low pressure	p_0	Omega PXM02MD0-040BARGV	0 to 40.0 bar	± 0.02 bar
flow rate	Q_1 , Q_2	VSE RS 400/32	1.0 to 400 l/min 0.5% MV*	
speed	ω	Rheintacho SDN4 (in mod1)	0.1 Hz to 20 kHz	
temperature	$\theta_0, \theta_1, \theta_2$	Testo type 13 PT100 class B	-50 to 400°C	±0.3°C

*accuracy for this sensor is defined as a percentage of the measured value (MV)

As mentioned before, the control angle of the transformer is controlled by the electric stepper motor. The load flow from port 2 is throttled by means of a needle valve that is also controlled by a stepper motor. The flow from this load valve passes through a heat exchanger, before it is routed back to the rest of the LPR.

5.2. Steady-state efficiency map

In order to describe the steady state performance of the FCT80, it has been exposed to a grid of measurement points, or samples, at different operating conditions. First of all, the pressure in the HPR and LPR (p_1 and p_0) is kept constant for the whole grid. Each sample consists of a combination of a certain pressure p_2 , controlled by the control angle, and flow rate Q_2 , controlled by the load valve. Once these conditions are set, the procedure has been to wait until the oil temperature at port 1 is $50\pm1^{\circ}$ C. This was achieved by controlling the cooling capacity of the heat exchanger. After some time, the temperature as well as all measured parameters are more or less stable, which means the transformer is operating in steady state. In this steady state, the sensor data is averaged over a period of 10 seconds. These average values per sample were used to calculate the efficiency maps shown in **Figure 8**. The black dots in these figures indicate the different sample points.

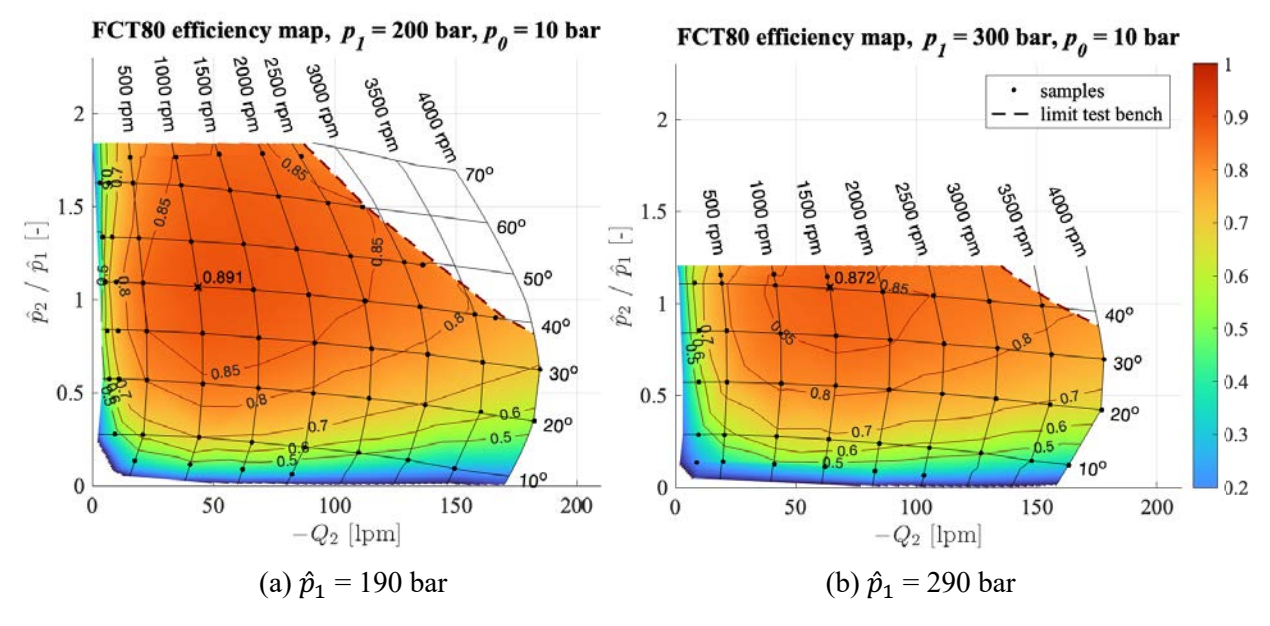


Figure 8: Measured steady-state efficiency map of the FCT80 at $p_0 = 10$ bar, $\theta_1 = 50$ °C

In **Figure 8**, the output flow rate at port $2(-Q_2)$ is shown on the x-axis, while the ratio between the output and input pressure (\hat{p}_2/\hat{p}_1) in shown on the y-axis. The maximum ratio of 1.84 and 1.21 correspond to a maximum output pressure \hat{p}_2 of 350 bar, which is the setting of the internal pressure relief valve. The somewhat horizontal lines are drawn at different control angles of the machine, while the vertical lines show different rotational speeds of the rotor. For this transformer, the maximum control angle is 70° and the maximum speed is 4000 rpm. The test bench is limited in terms of the maximum power that can be supplied to the transformer. The black dashed line shows the limit of the supply pump at the chosen HPR-pressure.

The face colour and other lines in **Figure 8** represent the measured steady state efficiency of the unit. The figures show that the efficiency of the transformer is very similar for the two different supply pressures. Overall, the efficiency is more than 0.7 for most of the center part of the field of operation. The maximum efficiency of 0.891 was measured at 40°, 1000 rpm, with a supply pressure of 200 bar. Looking at the edges of the efficiency map, we find that for low control angles and low rotor speeds, the efficiency decreases.

6. CONCLUSION

The introduction of CPR-systems and secondary control methods, have the potential to significantly reduce energy losses that are typically associated with current hydraulic systems. Hydraulic transformers can play a crucial role in the realisation of such systems. Since there are no commercially available hydraulic transformers, the FCT80 was developed as a new prototype transformer.

To describe the performance of the FCT80, a general definition for the power loss and efficiency of hydraulic transformers has been derived. The derived definitions describe the hydraulic input and output power of a transformer with respect to the minimum energy state of the CPR-system that the machine is part of. These definitions also take the compressibility of the oil into account.

For pumps and motors, it is common practice to divide the overall power loss into volumetric and mechanical losses based on the displacement volume of the tested unit. This approach was also used in an attempt to divide the overall transformer losses into volumetric and mechanical losses. However, since there is no known method to measure the actual displacement volume of an IHT for each possible control setting, the proposed equations for the division of losses are not applicable to the experimental measurements.

A specifically designed test setup was used to measure the steady state performance of the FCT80. The results are shown for two different supply pressures. For the measured samples, a peak efficiency of 0.891 was found. Furthermore, a large part of the field of operation was found to have an efficiency of 0.7 or higher, with decreasing efficiency for low control angles and low rotor speeds.

NOMENCLATURE

δ	Control angle	rad	subscripts	
η	Efficiency		0	low pressure rail
θ	Temperature	°C	1	high pressure rail
ω	Rotational velocity	rad/s	2	load pressure
\overline{K}_{S}	Average isentropic bulk modulus (1.76e9)	Pa	i	port index $(0,1,2)$
D	Displacement volume	m ³ /rad	in	input
P	Power	W	loss	loss
p	Absolute pressure	Pa	max	maximum
\hat{p}	Pressure relative to p_0	Pa	min	minimum
Q	Flow rate	m^3/s	out	output
T	Torque	Nm	Q	flow rate
V	Volume	m^3	T	torque
ΔV	Displacement volume per piston per rev.	m^3	th	theoretical
\boldsymbol{Z}	Number of pistons			

REFERENCES

- [1] Love, L. J., Lanke, E., and Alles, P. Estimating the impact (energy, emissions and economics) of the US fluid power industry. *Oak Ridge National Laboratory, Oak Ridge, TN*, 2012. doi:10.2172/1061537.
- [2] Vael, G. E., Achten, P. A., and Fu, Z. The Innas Hydraulic Transformer: the key to the hydrostatic common pressure rail. Technical report, SAE Technical Paper, 2000. doi:10.4271/2000-01-2561.
- [3] Linjama, M., Vihtanen, H.-P., Sipola, A., and Vilenius, M. Secondary controlled multi-chamber hydraulic cylinder. In *The 11th Scandinavian International Conference on Fluid Power, SICFP'09*, 2009.
- [4] Achten, P., Vael, G., and Heybroek, K. Efficient hydraulic pumps, motors and transformers for hydraulic hybrid systems in mobile machinery. In 1. *VDI-Fachkonferenz Getriebe in Mobilen Arbeitsmaschinen, Friedrichshafen, DE, 7.-8. Jun, 2011*, pages 1-19. VDI-Wissens- forum, 2011. diva2:1051356.
- [5] Heybroek, K., Vael, G. E. M., and Palmberg, J.-O. Towards resistance-free hydraulics in construction machinery. In *8th International Fluid Power Conference, Germany, Dresden*, volume 2, pages 123-138, 2012. diva2:1051345.
- [6] Shen, W., Jiang, J., Su, X., and Karimi, H. R. Energy-saving analysis of hydraulic hybrid excavator based on common pressure rail. *The Scientific World Journal*, 2013. doi:10.1155/2013/560694.
- [7] Siefert, J. and Li, P. Y. Optimal control and energy-saving analysis of common pressure rail architectures: HHEA and STEAM. In *BATH/ASME 2020 Symposium on Fluid Power and Motion Control*. American Society of Mechanical Engineers, 2020. doi:10.1115/FPMC2020-2799.
- [8] Achten, P., Fu, Z., and Vael, G. Transforming futur hydraulics: a new design of a hydraulic transformer. In *The Fifth Scandinavion International Conference on Fluid Power, SICFP'97*, page 287, 1997.
- [9] Li, X., Yuan, S., Hu, J., and Lv, J. Mathematical model for efficiency of the hydraulic transformer. In 2009 Asia-Pacific Power and Energy Engineering Conference, pages 1-5. IEEE, 2009. doi:10.1109/APPEEC.2009.4918475.
- [10] Zhou, J., Jing, C., and Wu, W. Energy efficiency modeling and validation of a novel swash platerotating type hydraulic transformer. *Energy*, 193, 2020. doi:10.1016/j.energy.2019.116652.
- [11] Achten, P., Potma, J., Achten, S., Achten, J., and Mommers, R. The design of the FCT80 hydraulic transformer. In *The 18th Scandinavion International Conference on Fluid Power, SICFP'23*, 2023.
- [12] Achten, P., Mommers, R., Nishiumi, T., Murrenhoff, H., Sepehri, N., Stelson, K., Palmberg, J.-O., and Schmitz, K. Measuring the losses of hydrostatic pumps and motors; a critical review of

- ISO4409:2007. In *BATH/ASME 2019 Symposium on Fluid Power and Motion Control*. American Society of Mechanical Engineers, 2019. doi:10.1115/FPMC2019-1615.
- [13] Williamson, C. and Manring, N. A more accurate definition of mechanical and volumetric efficiencies for Digital Displacement® pumps. In *BATH/ASME 2019 Symposium on Fluid Power and Motion Control*. American Society of Mechanical Engineers, 2019. doi:10.1115/FPMC2019-1668.
- [14] Li, P. Y. and Barkei, J. Hydraulic effort and the efficiencies of pumps and motors with compressible fluid. In *BATH/ASME 2020 Symposium on Fluid Power and Motion Control*. American Society of Mechanical Engineers, 2020. doi:10.1115/FPMC2020-2801.
- [15] Schänzle, C. and Pelz, P. F. Meaningful and physically consistent efficiency definition for positive displacement pumps continuation of the critical review of ISO4391 and ISO4409. In *BATH/ASME 2021 Symposium on Fluid Power and Motion Control*. American Society of Mechanical Engineers, 2021. doi:10.1115/FPMC2021-68739.
- [16] Werndin, R., Achten, P., Sannelius, M., and Palmberg, J.-O. Efficiency performance and control aspects of a hydraulic transformer. In *The 6th Scandinavion International Conference on Fluid Power, SICFP'99*, pages 395-407, 1999.
- [17] Werndin, R. Efficiency performance and control aspects of a hydraulic transformer. Linköping University, Dept. of Mechanical Engineering, 1999. Master Thesis.
- [18] Toet, G., Johnson, J., Montague, J., Torres, K., and Garcia-Bravo, J. The determination of the theoretical stroke volume of hydrostatic positive displacement pumps and motors from volumetric measurements. *Energies*, 12(3):415, 2019. doi:10.3390/en12030415.